

IOP Conference Series: Materials Science and Engineering

PAPER • **OPEN ACCESS**

Summertime thermal regime of water downstream of the Krasnoyarsk hydroelectric power plant

To cite this article: N Ya Shaparev and E V Bondarenko 2019 *IOP Conf. Ser.: Mater. Sci. Eng.* **537** 062085

View the [article online](#) for updates and enhancements.



IOP | ebooks™

Bringing you innovative digital publishing with leading voices to create your essential collection of books in STEM research.

Start exploring the [collection](#) - download the first chapter of every title for free.

Summertime thermal regime of water downstream of the Krasnoyarsk hydroelectric power plant

N Ya Shaparev^{1,2} and E V Bondarenko^{1,2}

¹ Federal Research Center Krasnoyarsk Science Center of the SB RAS, Krasnoyarsk, 660036, Russia

² Siberian Federal University, Krasnoyarsk, 660041, Russia

E-mail: jenia.b123@yandex.ru

Abstract. Summertime hydrothermal regime of the Yenisei River downstream of the Krasnoyarsk hydroelectric power plant is modeled based on a deterministic approach. To that end, the Fourier equation is used and the following physical processes contributing to the heat exchange between water and the surroundings are taken into consideration: absorption of direct and scattered solar radiation by water, absorption of downwelling thermal infrared radiation from the atmosphere by water surface, thermal infrared radiation back from the water surface, convection of heat and heat loss due to evaporation of water. A clearskies river thermal regime under no wind is studied in a 124-km stream reach below the power plant and the obtained results are compared against temperatures recorded at gauging stations.

1. Introduction

The Yenisei is the largest river in Russia in terms of runoff (624.41 km³/year). Water temperature and the streamflow velocity of the river have changed after commissioning a series of hydroelectric power plants, referred to as the Yeniseisky HPP Cascade (Sayano-Shushenskaya HPP, Mainskaya HPP, and Krasnoyarsk HPP). Changes in the temperature pattern entail changes in hydrological conditions of the river (e.g. absence of an ice crust) and biochemical processes (the growth of river flora and fauna). This inevitably has affected the environmental situation in the nearby areas. Krasnoyarsk HPP (second largest after Sayano-Shuchenskaya HPP) is the major anthropogenic factor influencing the Yenisei River and the area near the city of Krasnoyarsk. In this paper we study summer thermal regime of the Yenisei River downstream of the Krasnoyarsk HPP.

2. Mathematical modeling

The hydrothermal river regime can be described by a second-order Fourier equation [1-3]:

$$\frac{\partial T_w(x, t)}{\partial t} = -V(x) \frac{\partial T_w}{\partial x} + \lambda \frac{\partial T_w^2}{\partial x^2} + \frac{W(t) B(x)}{\rho c S(x)}. \quad (1)$$

Here c is the specific thermal capacity of water, T_w - the cross-sectional average water temperature, t (hour) - the time, x (km) - the distance from of the dam, λ - the heat conductivity coefficient, $B(m)$ - the stream width, V (km/h) - the average streamflow velocity found as the ratio between the water discharge through the dam body Q (m³/sec) and the stream cross-section S (m²):



$$V = \frac{Q}{S}. \quad (2)$$

$W(t)$ is the total surface heat flux equal to:

$$W(t) = W_s + W_a - W_w + W_c - W_e, \quad (3)$$

where W_s is *solar* radiation absorbed by water; W_a is atmospheric TIR absorbed by water; W_w is TIR from water surface to the atmosphere; W_c is convective heat transfer, and W_e is the loss of heat due to evaporation.

In the system of *coordinates* moving at a velocity $V(x)$ Equation (3) is rewritten as

$$\frac{dT_w(t)}{dt} = \frac{W(t)}{pc} \frac{B(x(t))}{S(x(t))}, \quad (4)$$

$S/B \approx d$ is the mean stream channel depth.

Solution of (4) is found from the expression

$$T_w(t) = \frac{1}{pcd} \int_{t_0}^t W(t) dt + T_w(0, t_0). \quad (5)$$

Here $T_w(0, t_0)$ is the *outflow* temperature of water leaving the dam.

3. Physical modeling

3.1. Solar radiation

Solar radiation reaching the Earth's atmosphere consists of direct solar radiation attenuated while going through the atmosphere and the direct solar radiation scattered in the atmosphere.

The power of extraterrestrial solar radiation incident on the Earth's atmosphere equals [4]

$$S = S_0 E \cos \theta, \quad (6)$$

where $S_0 = 1367 \text{ W/m}^2$ is the *solar* constant, E - the eccentricity correction factor, θ - the zenith angle

$$\cos \theta = \sin \varphi \cdot \sin \delta + \cos \varphi \cdot \cos \delta \cdot \cos \Omega, \quad (7)$$

where φ is the geographic latitude of the location and δ is solar declination depending on the time of the year. So, on July 3, 2016 solar declination was $\delta = 23.06^\circ$ and $E = 0.966$ [5]. For the Krasnoyarsk HPP we have $\varphi = 55.94^\circ$.

$$\Omega = \omega t, \quad (8)$$

where Ω is the hour angle, t - the time, ω - the angular velocity of the Earth's rotation around its axis.

From expressions (6) and (7) it follows that

$$S = S_0 E (A + B \cos \omega t), \quad (9)$$

where $A = \sin \varphi \cdot \sin \delta$, $B = \cos \varphi \cdot \cos \delta$.

The *sunrise* and sunset time equation is determined as

$$\cos \omega t_0 = -\tan \varphi \cdot \tan \delta = -\frac{A}{B}. \quad (10)$$

Equation (10) yields two values for the hour angle: the negative root $-\omega t_0$, refers to the sunrise and the positive one, ωt_0 , to the sunset. Solving this equation for our conditions yields $t_b = 4:08$ the time of sunrise and $t_s = 21:36$ the time of sunset. Hence the day length is 17:28 hours and the true noon (t_n) is at 12:52 local time.

Since t is the time from noon, we further have

$$\cos \omega t = \cos \left(\frac{\pi}{12} (t - t_n) \right). \quad (11)$$

Temporal behavior of *extraterrestrial* solar power is shown in figure 1 (Curve 1). So, solar power at true noon is $S = 1100 \text{ W/m}^2$.

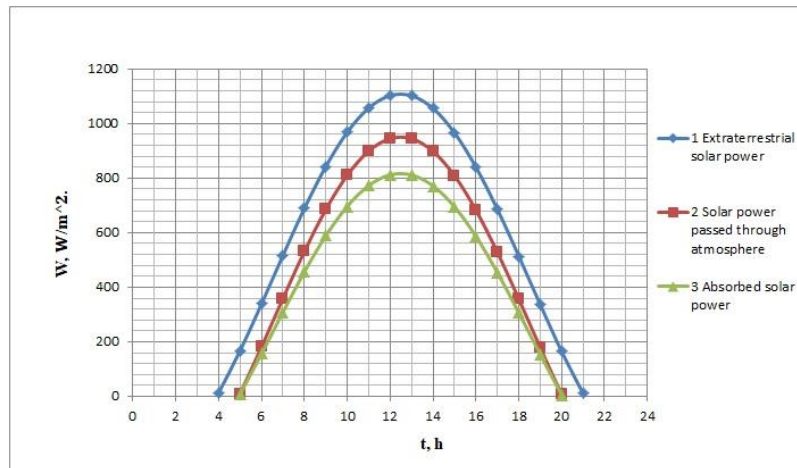


Figure 1. Temporal dependence of solar power.

Only part of solar radiation reaches the Earth's surface, the rest is scattered and absorbed by molecules of various gases, water droplets, ice crystals and aerosol impurities present in the atmosphere. Attenuation of a light beam propagating in absorbing medium obeys the Bouguer-Lambert-Beer law. According to this law the radiation power reaching the water surface is

$$S' = S \cdot \exp \left(-\frac{\tau_0}{\cos \theta} \right), \quad (12)$$

where τ_0 is the optical thickness of atmosphere for $\cos \theta = 1$ ($\theta = 0$, which corresponds to the sun in zenith). For $\tau_0 \ll 1$ expression (12) can be expanded in Taylor series

$$S' = S_0 E \cos \theta - S_0 E \tau_0. \quad (13)$$

Temporal behavior of the solar power passed through atmosphere is shown in figure 1 (Curve 2). So, at true noon it is $S' = 900 \text{ W/m}^2$.

Upon reaching a plane water surface, solar radiation is partially reflected. The reflection coefficient R is calculated by the Fresnel's formula

$$R = \frac{1}{2} \left[\frac{\sin^2(\varphi - i)}{\sin^2(\varphi + i)} + \frac{\tan^2(\varphi - i)}{\tan^2(\varphi + i)} \right], \quad (14)$$

where $\varphi = (90 - \theta)$ is the angle of incidence and the angle of refraction i is found from the relation

$$\sin i = \frac{\sin \varphi}{n}, \quad (15)$$

where $n=1.33$ is the refractive index of clear water.

Dependence of the reflection coefficient on the angle of incidence is shown in figure 2.

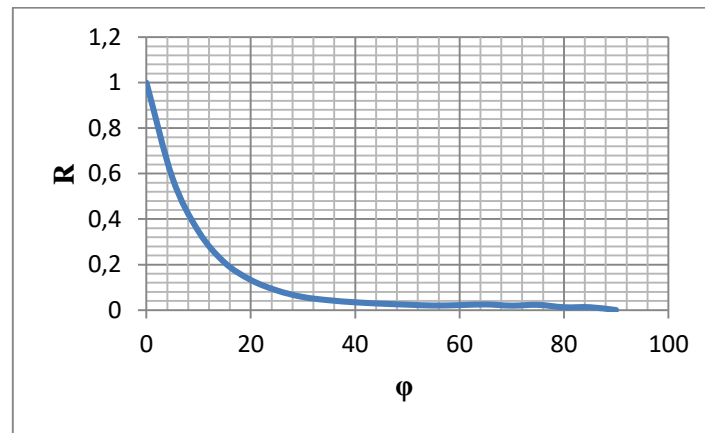


Figure2. Reflection coefficient versus angle of incidence.

The part of solar energy that has successfully penetrated through the atmosphere and has not been reflected by water surface ($1-R$) is absorbed by water at a depth of about one meter thereby increasing its temperature [6]. Thus the solar power absorbed by water is

$$W_s = (1 - R)S', \quad (16)$$

Temporal behavior of the absorbed solar power is shown in figure 1 (Curve 3). At true noon $W_s = 811 \text{ W/m}^2$.

3.2. Thermal radiation

3.2.1. Emission from water. The Stefan-Boltzmann law states that the heat energy emitted by an absolutely black body is proportional to the fourth power of its temperature

$$A = \sigma T^4, \quad (17)$$

where T is temperature in degrees Kelvin and σ is the Stefan-Boltzmann constant. According to Wien's displacement law, the black-body radiation curve peaks at a wavelength λ_{\max} , inversely proportional to the absolute temperature T .

$$\lambda \approx \frac{0,29}{T}. \quad (18)$$

For $T = 283^\circ\text{K}$, $\lambda \approx 10\mu\text{m}$. This wavelength is absorbed at a depth of $100 \mu\text{m}$ and since it is much less than the total water depth the energy emitted by water, according to the Stefan-Boltzmann law, is

$$W_w \simeq \varepsilon_w \sigma (273 + T_w)^4, \quad (19)$$

where $\varepsilon_w = 0.995$ [7] is the emission coefficient of water. Expanding in Taylor's series yields

$$W_w \simeq A + BT_w, \quad (20)$$

Where $A=313.36$, $B=4.59$.

Energy emitted by water on July 3, 2016 at night temperature $T_2 = 7^\circ\text{C}$ and day temperature $T_2 = 20^\circ\text{C}$ was $W_{w1} = 346 \text{ W/m}^2$ and $W_{w2} = 413 \text{ W/m}^2$, respectively.

3.2.2. Atmospheric emission. Water surface absorbs atmospheric thermal radiation and gets warmer. Energy emitted by the Earth's atmosphere obeys the same Stefan-Boltzmann law.

$$W_a \simeq \varepsilon_a \sigma (273 + T_a)^4. \quad (21)$$

On July 3, 2016 the atmospheric temperature was $T_{a1} = 15$ day and $T_{a2} = 25$ at night.

The atmospheric emission coefficient ε_a was found as [8]:

$$\varepsilon_a = 1 - 0.4 \cdot \exp\left(-\frac{100e_a}{T_a + 273}\right), \quad (22)$$

where e_a – the pressure of water vapor:

$$e_a = \frac{H}{100} e_s, \quad (23)$$

e_s – the pressure of saturated vapor:

$$e_s = 6.1 \cdot \exp\left(\frac{17.27 \cdot T_a}{273 + T_a}\right). \quad (24)$$

H is the atmospheric humidity.

Table 1 summarizes our results on atmospheric emission calculations

Table1. Atmospheric emission characteristics.

	$T_{a2}, ^\circ\text{C}$	$H, \%$	e_s, mBar	e_a, mBar	ε_a	$W_a, \text{W/m}^2$
Night	15	85	14.99	12.74	0.995	388.21
Day	25	45	25.97	11.68	0.992	443.60

3.3. Heat exchange between water surface and atmosphere

3.3.1. Evaporation. The energy spent on water evaporation, W_e , is estimated as [6]:

$$W_e = \rho L f(w)(e_s - e_a), \quad (25)$$

where $L=2.26 \cdot 10^6 \text{ J/kg}$ is the latent heat of evaporation, $f(w)$ is the wind function determined as

$$f(w) = a + bw. \quad (26)$$

w is the wind velocity, $a \simeq 3 \cdot 10^{-9}$, $b \simeq \left(\frac{1}{6}\right) \cdot 10^{-9}$.

When the pressure of water vapor exceeds that of saturated water vapor, water evaporates and the water temperature drops. In a reverse situation we deal with condensation of water vapor and the water temperature increases.

Table 2. Energy spent on water evaporation.

	$w = 0 \text{ m/sec}$	$w = 1.6 \text{ m/sec}$
	$W_e W / m^2$	
Night	15.25	16.62
Day	96.88	105.57

3.3.2. *Convection.* Convective heat exchange between water surface and atmosphere is estimated as [6]:

$$W_c = 0,61 \rho L f(w) \cdot (T_w - T_a). \quad (27)$$

If $T_w < T_a$ water temperature will grow due to convection and it will go down if on the contrary.

Table 3. Convective heat exchange.

	$w=0 \text{ m/sec}$	$w= 1.6 \text{ m/sec}$
	$W_c W \cdot m^{-2}$	
Night	33.09	36.06
Day	20.67	22.54

4. Results

We consider a 124-km reach of the Yenisei River downstream the dam of the Krasnoyarsk HPP. The reach is divided by 4 cross-section lines at (0.5, 40, 77, 124 km) with gauging stations at the first, second and forth section lines to measure water temperature. The first station is located next to the dam ($x = 0.5$ km) and measures water temperature leaving the dam. The other two are located at 40 km and 124 km downstream. Streamflow velocity is assumed constant from section to section and is found from Eq. (1) at $Q = 2900 \text{ m}^3 \text{sec}^{-1}$. The S is equal to the cross-sectional area of the downstream lowest reach section. Flow time between section lines is found as the section-to-section distance divided by the flow velocity. Temperature measurements at the gauging stations are taken at time, t_g (at 08:00 and 20:00 hour). Water leaves the dam at time $t_0 = t_g - t_i$ where t_i is the length of time within which water from the dam reaches a cross-section line. Water temperature was computed using Eq. (5) which now has the form:

$$T_w(t) = \frac{1}{\rho c d} \sum_{i=2}^4 W_i \Delta t_i + T_w(0, t_0), \Delta t_1 = t_i - t_{i-1}. \quad (28)$$

where i is the reach section number, Δt_i – the flow time between the $i - 1$ and i section lines, $W_i \Delta t_i$ – the energy received by water along each reach section. Power W_i depends on day or night time, water and atmospheric temperature, water vapor pressure, and humidity. Morphometric and hydrophysical characteristics of the river reach sections are summarized in table 4.

Table 4. Morphometric and hydrophysical characteristics.

Cross-section line number	1	2	3	4
Dam-to-section line distance, [km]	5	40	77	124
Width B, [m]	520	830	580	450
Cross-sectional area S, [m ²]	1834	2254	2452	2513
Stream flow velocity, [km/hour]	5.7	4.6	4.3	3.7

Flow time between adjacent cross-section lines, Δt_i , [hours]		7.6	9.5	11.9
Relation B/S, [m^{-1}]		0.283	0.368	0.236
Tw July 3 at 08.00, °C	Calculated	7.8	8.7	10.1
	Measured	7.2	8.0	10
Tw July 3 at 20.00, °C	Calculated	9.0	9.9	10.3
	Measured	7.2	9.0	10.6

5. Conclusion

We have proposed a simple model for simulating summertime hydrothermal regime of a river based on calculation of water temperature in a co-ordinate system moving with water. The physically based estimation of water heat budget takes into account absorption of solar radiation by water surface, emission and absorption of atmospheric TIR by water, convective heating of water as well as heat loss due to evaporative processes. The temporal fluctuation pattern of direct and scattered solar radiation depends on the zenith angle and atmospheric absorption. The dominant water heating factor is solar radiation during daytime and atmospheric TIR at night. Water temperatures 124 km downstream of the Krasnoyarsk HPP on the Yenisei River computed using the proposed model with consideration of morphometric characteristics are close to the recorded temperatures observed at the gauging stations, which proves that the deployed physical-mathematical model provides an adequate description of the actual hydrothermal processes.

References

- [1] Sinokrot B A and Stefan H G 1993 Stream Temperature Dynamics *Measurements and Modelling, Water Resour* **7** 2299-112
- [2] Shaparev N Y and Shokin Yu I 2018 Modelling summer hydrothermal regime downstream the Krasnoyarsk HPP *Computational Technologies* **23(6)** 107–14
- [3] Shaparev N Y 2019 Modelling summer water temperature on the Yenisei River *Thermal Sciences* **23(2)** 1–8
- [4] Kondratyev K Y 1969 *Radiation in the atmosphere* (N.Y.: Acad. Press)
- [5] Iqbal M 1983 An Introduction to Solar Radiation Academic Press Canadian *Library of Congress Cataloging in Publication Data* p 132
- [6] Dingman S L 2015 *Physical Hydrology* (Waveland Press. Inc.)
- [7] Handcock R N, Torgersen C E, Cherkauer K A, Gillespie A R, Tockner K, Faux R N and Tan J 2012 *Thermal infrared remote sensing of water temperature in riverine hands capes. Fluvial Remote Sensing for Science and Management* ed Patrice E (John Wiley and Sons, Ltd.)
- [8] Iziomon M G *et al.* 2003 Downward Atmospheric Longwave Irradiance under Clear and Cloudy Skies *Measurement and Parametrization, J. Atmosph. SolarTerrestrialPhys.* **65 (10)** 1107-16